IRSTI 29.17.35 https://doi.org/10.26577/ijmph.20211526

NUMERICAL SIMULATION OF BIODIESEL AIR-BLAST ATOMIZATION AND FLOW DYNAMICS

Sh. Ospanova [1*], **G. Karybayeva** [1], **G. Partizan** [2], **G. Shinikulova** [1], **A. Aldibekova** [1] and **K. Rustemova** [1]

[1] *Almaty Technological University, Almaty, Kazakhstan*

[2] *Joint-Stock Company "National Center of Space Research and Technology", Almaty, Kazakhstan*

Email: s.osspanova@gmail.com

(Received 10 October 2026; revised 23 October 2026; accepted 5 November 2026)

Abstract. The transition to low-emission energy systems has increased interest in biodiesel as a viable alternative to fossil fuels to reduce greenhouse gas emissions. This study numerically investigates two-phase reacting flows and the atomization of high-viscosity biofuel in a coaxial air-blast atomizer. A 2D axisymmetric computational fluid dynamics model uses a coupled Eulerian–Lagrangian approach and incorporates the Realizable k- turbulence model and hybrid K-H/R-T criteria for primary and secondary droplet breakup. The results show that strong velocity gradients at the nozzle exit generate high turbulence kinetic energy and relative velocities in the shear layer. Although increased fuel viscosity extends the continuous liquid core length compared to conventional diesel fuels, intensive secondary breakup effectively produces a fine-droplet fraction at the spray periphery, significantly enhancing evaporation rates. These findings establish a robust computational foundation for modeling high-viscosity fuel atomization and serve as a reliable digital tool for optimizing injector design, improving combustion efficiency, and mitigating pollutant formation in modern power plants.

Keywords: biodiesel, air-blast atomization, Sauter mean diameter, turbulent kinetic energy, numerical modeling.

INTRODUCTION

The modern energy development vector, aimed at transitioning to environmentally friendly, renewable energy sources, has driven strong interest in biodiesel (methyl esters of fatty acids) as a promising alternative to petroleum diesel fuel in engines and thermal power plants. Adopting biodiesel substantially reduces anthropogenic emissions of soot, sulfur oxides, and greenhouse gases while supporting a near-neutral carbon balance.

As shown in Fig. 1, the global primary energy consumption is presented, highlighting key trends in replacing traditional fossil fuels with alternative energy sources. As shown in the figure, the renewable energy and bioresources segment, including biodiesel, holds a predominant share (38%), far exceeding the fossil oil sector (11%) [1, 2, 3]. This three-fold ratio reflects the global transition to cleaner motor fuels. Unlike petroleum diesel, which has a high carbon footprint and significant sulfur content, biodiesel, as part of the renewable sector, offers a neutral balance of CO_2 emissions and virtually no sulfur oxides (SOx).

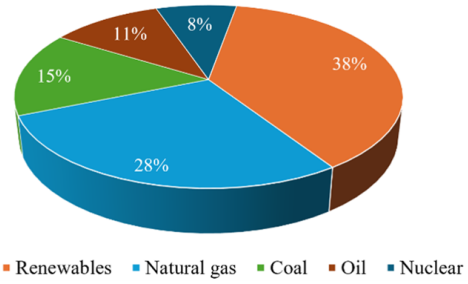


Figure 1 - Structure of global primary energy consumption by energy source type, highlighting the share of renewable energy sources and biofuels (2024–2025)

As shown in Fig. 2, the modern transport sector is based on data from the International Energy Agency [4, 5]. The market remains dominated by traditional petroleum-based products: fossil-derived diesel (76.5%) and gasoline (18%). Environmentally friendly biofuels (biodiesel, Bio-

 © 2026 Al-Farabi Kazakh National University

FAME, HVO) account for approximately 4.2%, while electric propulsion and natural gas-based fuels (EV, CNG, LNG) together make up 1.3%. This breakdown reflects the current share of biocomponents and highlights their significant expansion potential, which could help decarbonize the transport energy sector.

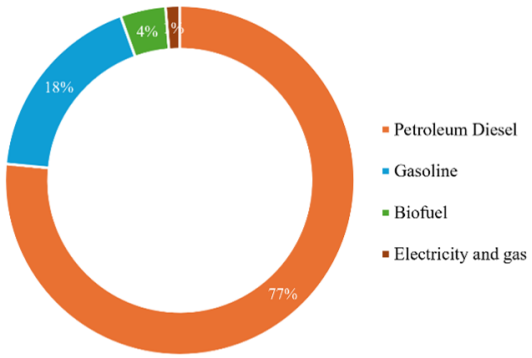


Figure 2 - Structure of motor fuel consumption in the transport sector, with the share of biofuels highlighted (2024–2025)

However, biodiesel's large-scale practical implementation is significantly constrained by its specific thermophysical properties. Compared with conventional mineral diesel fuel, biodiesel has higher kinematic viscosity (1.5–2 times that of its petroleum-based counterpart), higher surface tension, greater density, and lower volatility [6]. These differences adversely affect jet hydrodynamics and mixture formation processes. Under conditions of using standard hydraulic mechanical nozzles, the high viscosity of biodiesel prevents the intensive development of capillary waves, which leads to the formation of a coarsely dispersed spectrum of droplets [7], a delay in phase transformations (evaporation) [8], incompleteness of the chemical reaction and, as a consequence, a decrease in the thermal efficiency of the unit [9, 10].

An effective method for intensifying the breakup of highly viscous liquid media is air-blast atomization (Fig. 3).

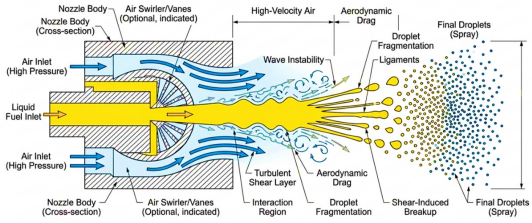


Figure 3 - Schematic of the primary and secondary breakup processes of a liquid jet during air-blast atomization

In devices of this type, primary and secondary fragmentation of a liquid jet (or film) occurs due to the transfer of momentum and kinetic energy from a high-speed shear flow of atomizing air. This ensures finely dispersed spray with a low Sauter mean diameter, even at moderate fuel supply pressures.

The process relies on the aerodynamic destructive effect of high-speed air flows on a liquid jet or film, ensuring effective fragmentation into a finely dispersed torch. An air-blast atomizer design includes a central channel that supplies liquid fuel at relatively low pressure, along with peripheral nozzle passages that deliver atomizing air at high subsonic or supersonic velocities. In the aerodynamic interaction zone at the nozzle exit, the gas stream transfers kinetic energy to the liquid phase. This causes the continuous fuel stream to break up into unstable filaments that subsequently fragment into droplets, forming a homogeneous, finely dispersed fuel-air spray [11].

Furthermore, intensification of combustion processes and enhancement of the environmental efficiency of bioenergy systems are achieved not only through hydrodynamic optimization of fuel atomization but also through several complementary methods: catalytic modification of fuels using functional nanomaterials and metallic nanostructures [12], synthesis and integration of two-dimensional carbon-based catalytic structures [13], treatment of fuel streams with electromagnetic and ultrasonic fields, and use of viscosity-reducing additives. This highlights the comprehensive nature of research aimed at improving promising alternative energy systems.

Because of the high degree of local nonstationarity and the spatial limitations of the pri-

mary disintegration zone of a two-phase jet inside the nozzle mixing chamber, direct experimental measurement of flow parameters is significantly complicated. Consequently, computational fluid dynamics (CFD) methods play a crucial role. Numerical modeling enables detailed investigation of interphase aerodynamic interactions, determination of the spatial distribution of the dispersed phase (including droplet size spectrum characteristics), and optimization of both the atomizer's geometric and operational parameters.

The approach presented in this work, based on a combined Eulerian-Lagrangian description of a two-phase flow within a 2D axisymmetric framework, offers the following key advantages:

- It integrates an Eulerian approach for describing the macrostructure of the continuous liquid core with Lagrangian tracking of individual droplet trajectories, velocities, and size evolution;

- It enables the high-precision calculation of local physical parameters that are inaccessible via direct optical measurements (such as velocity gradients, interfacial interaction zones, and the distribution of turbulent kinetic energy);

- It ensures high accuracy in predicting the Sauter mean diameter of droplets and their polydisperse composition throughout the entire length of the spray plume;

- The 2D axisymmetric model provides precise resolution of shear layers and near-nozzle regions while maintaining optimal computational efficiency.

This study quantitatively investigates the thermophysical and structural-kinematic patterns of biodiesel jet disintegration in a coaxial air-blast atomizer. The results provide a reliable scientific and methodological basis for optimizing injector design parameters and combustion modes for alternative fuels.

Materials and Methods

A combined Eulerian-Lagrangian approach provides a detailed mathematical description of the hydrodynamics of two-phase flow in a coaxial atomizer. Within this framework, the carrier continuous medium (gas flow and primary liquid core) is treated in the Euler formulation, solving the Reynolds-averaged Navier–Stokes equations and the conservation laws of mass, momentum, and energy, closed with the two-parameter Realizable $k-\varepsilon$ turbulence model.

The dispersed phase (an ensemble of biodiesel droplets) is modeled in a Lagrangian formulation by discrete tracking of individual particle trajectories, taking into account the interphase exchange of mass, momentum, and heat, as well as the dynamic processes of primary and secondary breakup based on hybrid Kelvin–Helmholtz and Rayleigh–Taylor instability criteria. This approach enables precise resolution of local velocity gradients, shear-stress zones, and the evolution of the polydisperse composition throughout the spray plume.

In this study, the processes of biodiesel droplet evaporation, chemical heat release, and combustion are explicitly accounted for via source terms in the conservation equations for mass, momentum, and internal energy, within an Eulerian–Lagrangian framework. The Realizable k-ε turbulence model is chosen to capture the specifics of high-speed air-blast atomization and combustion.

The combined influence of jet breakup, phase transition, and exothermic reactions forms sharp velocity gradients, streamline curvature, and intense volumetric expansion of the gas in the shear layer. Under such conditions, the standard k-ε model tends to produce an unphysical overestimation of turbulent kinetic energy. The Realizable k-ε model overcomes this limitation through a modified turbulent viscosity formulation incorporating a variable coefficient C_μ and the application of realizability constraints, which ensure high computational stability.

Although the Reynolds Stress Model (RSM) accounts for anisotropy in detail, it is characterized by high computational stiffness, grid sensitivity, and convergence difficulties when coupled with a Lagrangian droplet tracking model and combustion source terms. Consequently, the Realizable k-ε model provides an optimal balance between computational efficiency, numerical sta-

bility, and the physical accuracy of the results.

Equations

The mathematical formulation governing liquid fuel droplet atomization, evaporation, and combustion incorporates the conservation laws of mass, momentum, internal energy, and chemical species concentration for a two-phase reacting flow [14, 15, 16].

Accordingly, the mass conservation (continuity) equation for the fuel-air mixture is expressed as follows:

$$\frac{\partial \rho}{\partial t} + \operatorname{div}(\rho \mathbf{u}) = S_{\text{mass}}, \tag{1}$$

where $\mathbf{u}$ denotes the fluid velocity vector, and S_{mass} represents the local rate of change.

The mixture momentum conservation equation for the two-phase flow is expressed as:

$$\rho \frac{\partial \mathbf{u}}{\partial t} + \rho(\operatorname{grad}\mathbf{u})\mathbf{u} = \operatorname{div}\xi + \rho\mathbf{g} + S_{\text{mom}}, \tag{2}$$

where S_{mom} represents the local rate of momentum change in the gas phase induced by droplet motion and interaction.

The conservation equation for internal energy of the mixture is expressed as:

$$\rho \frac{\partial E}{\partial t} = \tau : \mathbf{D} - \rho \operatorname{div}\mathbf{u} - \operatorname{div}\mathbf{q} + S_{\text{energy}}, \tag{3}$$

where $\mathbf{q}$ is the specific heat flux determined by Fourier's law, and S_{energy} is the source term accounting for the change in internal energy due to the presence and thermal interaction of the atomized liquid phase.

The conservation equation for the mass concentration of chemical component m in the two-phase reacting flow is expressed as:

$$\frac{\partial(\rho c_m)}{\partial t} = -\frac{\partial(\rho c_m u_i)}{\partial x_i} + \frac{\partial}{\partial x_i}\left(\rho D_{c_m}\frac{\partial c_m}{\partial x_i}\right) + + S_{\text{mass}}, \tag{4}$$

where ρ_m is the mass density of component m, and ρ is the total mass density.

In air-blast atomization systems, a high-velocity airflow interacts with a continuous liquid biofuel film or jet, causing aerodynamic shear forces to break it up. To simulate the primary and secondary breakups, the coupled Kelvin–Helmholtz and Rayleigh–Taylor (KH-RT) instability model is used [17].

The aerodynamic breakup of droplets is determined by the Weber number and the Ohnesorge number, which account for the increased viscosity and surface tension of the biofuel [18]:

$$We_g = \frac{\rho_g |\mathbf{u}_g - \mathbf{u}_d|^2 d_d}{\sigma}, \tag{5}$$

$$Oh_d = \frac{\mu_d}{\sqrt{\rho_d \sigma d_d}}, \tag{6}$$

where ρ_g and ρ_d are the densities of the gas and droplet phases; $\mathbf{u}_g$ and $\mathbf{u}_d$ are their velocity vectors; d_d is the droplet diameter; σ is the surface tension coefficient; and μ_d is the dynamic viscosity of the biofuel.

The characteristic breakup time τ_{KH} and the size distribution of daughter droplets, resulting from the growth of Kelvin–Helmholtz surface waves, are calculated using the following relations:

$$\tau_{\text{KH}} = \frac{3.726 B_1 r_d}{\Lambda_{\text{KH}} \Omega_{\text{KH}}}, \tag{7}$$

$$r_{\text{child}} = B_0 \Lambda_{\text{KH}}, \tag{8}$$

where Λ_{KH} and Ω_{KH} are the wavelength and growth rate of the fastest-growing Kelvin–Helmholtz wave, respectively; B_0 and B_1 are empirical constants. Secondary breakup, driven by the rapid acceleration or deceleration of droplets within a turbulent air stream, is described using Rayleigh–Taylor instability criteria.

A two-parameter Realizable k-ε turbulence model closes the Reynolds-averaged Navier-Stokes (RANS) equations and accurately models high-speed air jets, shear flows, and circulation zones in the combustion chamber. This model includes an improved expression for turbulent viscosity and a modified transport equation for the dissipation rate, providing high accuracy for swirling and jet flows [19, 20].

Computational domain and numerical setup

The computational domain is a two-dimensional (2D) axisymmetric model of a coaxial air-blast atomizer, where an Eulerian-Lagrangian approach describes the two-phase flow. The geometry includes a central channel for liquid biodiesel supply, surrounded by coaxial annular channels for high-velocity air that flows around the fuel jet. As the Liquid Volume Fraction distribution shows, a continuous, highly concentrated fuel core (red zone) forms near the nozzle exit along the axis of symmetry. The interaction of the high-speed gas flow with the jet surface creates strong shear stresses, causing wave formation and further disintegration of the solid core into droplets of different diameters (green and blue zones) (Fig. 4).

In the numerical model, we used a biodiesel fuel based on rapeseed methyl ester (RME B100) as the working liquid fuel. The density of the liquid phase was set within the range of 860–880 kg/m³, while the dynamic viscosity and surface tension coefficient were defined as functions of temperature, with an initial injection temperature of 300 K. The velocity of the atomizing air at the inlet was varied from 60 to 120 m/s (with an air supply gauge pressure of up to 0.5–1.0 bar), the airflow temperature ranged from 360 to 650 K. The pressure at the combustion chamber outlet was assumed to be equal to atmospheric pressure (1.013 bar).

To accurately reproduce the initial disturbances of the Kelvin-Helmholtz instability at the interface between the liquid fuel jet and the gas flow, an appropriate spatial resolution is required. To ensure high accuracy of the solution in areas of intense velocity gradients and changes in the volume fraction of phases, especially in the region of primary droplet breakup at the nozzle outlet and along the axis of symmetry, a structured computational grid with locally condensed elements was constructed. The selected cell size allows for the correct recording of the characteristics of interphase disturbances and the subsequent disintegration of the liquid jet.

Furthermore, to verify the reliability of the results, a grid independence study was conducted using three levels of grid resolution: coarse, baseline, and fine. The base mesh with a denser near-nozzle mesh was chosen as the optimal option, since it provides the best balance between the accuracy of predicting the droplet distribution and spray pattern dynamics on the one hand, and minimal computational costs on the other. A coarse mesh introduces excessive numerical diffusion, while a fine mesh leads to an unjustified increase in calculation time without a significant increase in the accuracy of the integral parameters. The conducted analysis confirmed the reliability and stability of the selected grid configuration.

To describe the liquid-phase dynamics in a gas flow, we used a Lagrangian particle-tracking model (Fig. 5).

This approach enables calculation of individual droplet trajectories, evaporation, and interphase heat and mass transfer with the surrounding medium. This ensures an accurate analysis of droplet spatial distribution, temperature profiles, and concentration fields in the torch, which is crucial for understanding fuel evaporation and combustion mechanisms and improving the accuracy of dispersed-phase modeling; a probabilistic droplet-collision model has been integrated. When droplet trajectories intersect, the model evaluates the interaction probability and accounts for processes such as coalescence (merging) and secondary breakup (fragmentation). Incorporating these effects significantly enhances the reliability of hydrodynamic simulations, providing a precise forecast of the evolution of the polydisperse droplet size distribution, evaporation rates, and the spatial structure of the fuel spray.

Results and Discussion

Using two-dimensional axisymmetric numerical modeling of coaxial air-jet atomization (Air-Blast Atomization) within the Euler-Lagrangian framework, we comprehensively analyzed the two-phase flow's thermophysical and structural-kinematic characteristics. The spatial distributions of key physical parameters detail the interphase-interaction mechanisms: from the for-

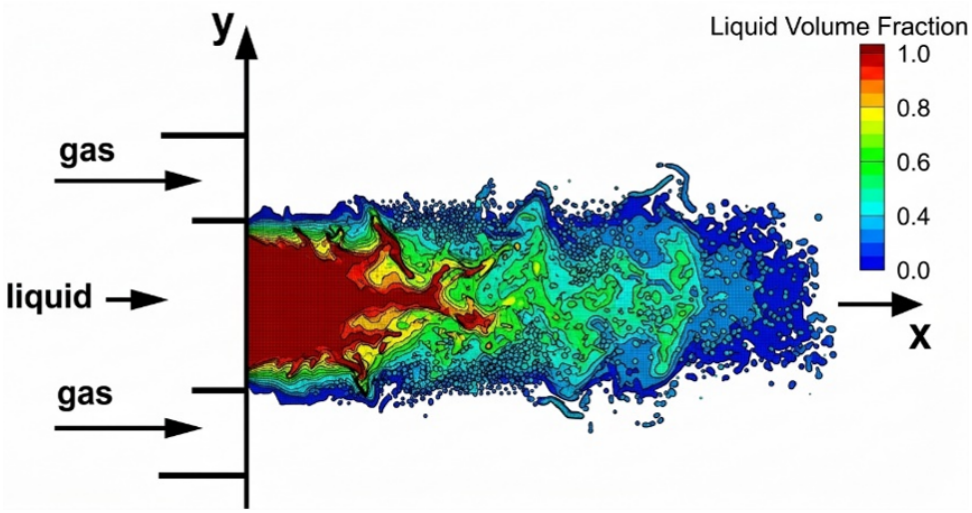


Figure 4 - Two-phase flow structure and liquid volume fraction distribution in a co-axial air-blast atomizer

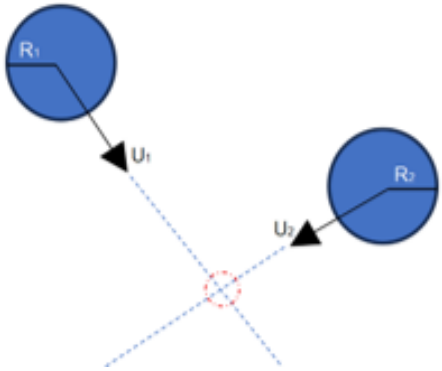


Figure 5 - Schematic diagram of the model of droplet tracking and their collisions in a two-phase flow

mation of a continuous, highly concentrated biodiesel core near the nozzle exit to the development of wave instability under strong aerodynamic shear stresses and the subsequent disintegration of the jet into droplets.

Fig. 6 shows the spatial distribution of the biodiesel droplet number density within a two-dimensional axisymmetric computational domain. This parameter characterizes the local concentration of the dispersed phase per unit control volume. The displayed isocontour plot reveals the spatial heterogeneity of the two-phase flow structure. The region of maximum values (highlighted in red along the axis of symmetry, y=0) is localized near the nozzle. This topology results from the primary breakup of the continuous biofuel jet core, driven by hydrodynamic shear forces and aerodynamic instabilities generated by a high-velocity co-flowing gas stream.

As kinetic energy dissipates and the phases' velocities equalize along the x-axis, the droplet number density relaxes monotonically (manifesting as a shift toward the green and blue ranges of the spectrum). The decrease in local droplet concentration away from the nozzle exit results from radial jet divergence, secondary disintegration, turbulent transfer, and aerodynamic dispersion of the dispersed phase in the carrier gas.

The observed spatial distribution of droplet number density and the breakup of the biodiesel jet core are qualitatively consistent with the fundamental principles of Eulerian-Lagrangian modeling for air-blast atomization, as described in the literature [21, 22]. However, unlike less viscous analogs, where the destruction of the liquid core and relaxation of the droplet density occur at shorter distances (x/d<5), in biodiesel (RMEB100), due to increased dynamic viscosity and surface tension, the length of the nozzle zone with a high concentration of the dispersed phase is 15–25% greater. This shifts the zone of maximum droplet density further downstream along the flow axis and requires a longer mixing length to achieve a homogeneous spray plume.

Fig. 7 shows the spatial distribution of the liquid volume fraction (L.V.F.) within a two-dimensional axisymmetric computational domain. This parameter characterizes the relative proportion of the computational cell volume oc-

cupied by the liquid phase. The contour plot clearly reveals the extent of a continuous, highly concentrated core of biofuel (the red zone, where L.V.F. $\approx$ 1) in the initial region of the flow, immediately downstream of the nozzle exit. The rapid decrease in the liquid-phase volume fraction along the torch length (transition to the green and blue regions) quantitatively confirms the high efficiency of aerodynamic dispersion, the involvement of droplets in a high-speed gas flow, and their intensive spatial redistribution.

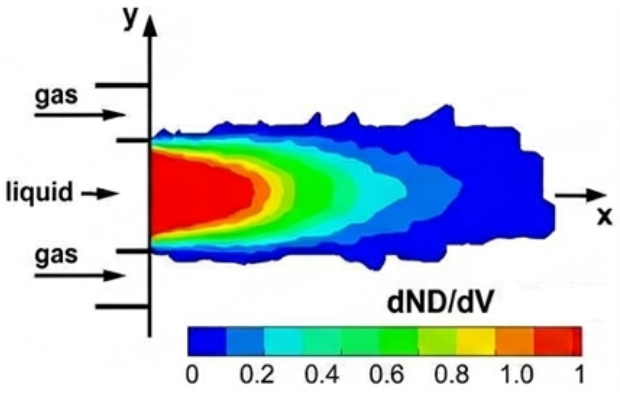


Figure 6 - Spatial distribution of the number density of biodiesel droplets in a two-dimensional axisymmetric computational domain

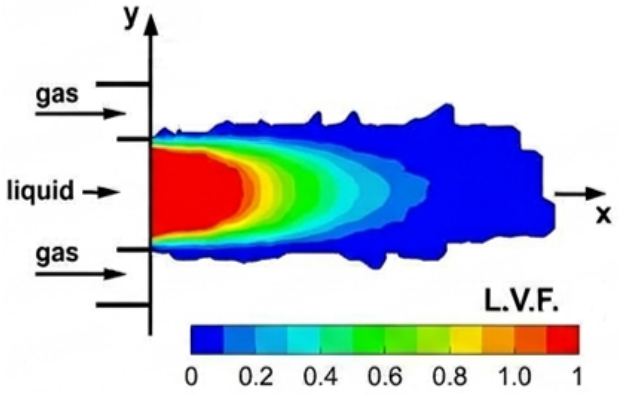


Figure 7 - Spatial distribution of liquid volume fraction (L.V.F.) of biodiesel in a two-phase flow

Fig. 8 shows the spatial distribution of the Sauter mean diameter (D_{32}) of biodiesel droplets in a two-phase flow. This parameter indicates atomization fineness and is defined as the ratio of total droplet volume to total droplet surface area.

The presented isofield clearly illustrates the spatial heterogeneity of the droplet size distribution within the spray plume. The maximum SMD values, reaching 1000 μm (red and orange regions, 500-1000 μm), are localized in the peripheral zones of intense hydrodynamic shear at the jet-high-speed gas interface, where large fragments and ligaments are primarily separated from the solid fuel core.

As secondary fragmentation develops under aerodynamic resistance and turbulent dissipation, droplet diameter decreases monotonically along the x-axis through intermediate values of 150-200 μm (green and yellow tones). A finely dispersed fraction with minimal SMD values in the 0-100 μm range (blue area) forms at the spray front and torch outer boundaries, which is key to accelerating interphase mass transfer, evaporation, and subsequent complete combustion of biofuel.

The observed spatial variation in the Sauter Mean Diameter (SMD) qualitatively agrees with visual and numerical analyses of fuel spray structures [23], as well as with contemporary developments in Eulerian-based modeling of turbulent flows using the Realizable k-ε model [24]. The distributions confirm that droplet size distribution development in the near-nozzle region depends critically on atomization intensity and aerodynamic phase interaction. At the same time, biodiesel's higher dynamic viscosity and surface tension (RMEB100) naturally enlarge droplets in the initial disintegration zone compared to traditional fuels, requiring a longer chamber to complete secondary fragmentation and stabilize the average Sauter diameter.

Fig. 9 shows the spatial distribution of the carrier-gas velocity magnitude (v_{gas}) within a two-dimensional axisymmetric computational domain. The maximum speed values in the range of 1.0-1.2 m/s (red and orange zones) are localized in coaxial peripheral channels at the nozzle exit (x=0). High velocity gradients at the phase interface generate strong aerodynamic shear stresses, which trigger wave instability and the primary breakup of the continuous biodiesel core.

As the flow moves along the x-axis, the kinetic energy of the gas dissipates due to turbulent mix-

ing and the entrainment of droplets into motion, which leads to a smoothing of the velocity profile:

- in the zone of intense interaction and wave formation, the velocity decreases to 0.6-0.8 m/s (green-yellow region);

- in the inner region of the fuel core and stagnant zones, the values are minimal and amount to 0-2 m/s (blue zone);

- in the far spray trail (x>0), the velocity field stabilizes at a level of 0.4-0.6 m/s.

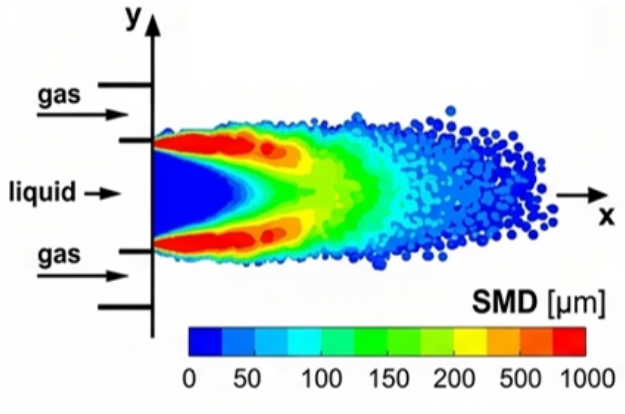


Figure 8 - Spatial distribution of the Sauter mean diameter (D_{32}) of biodiesel droplets in the computational domain

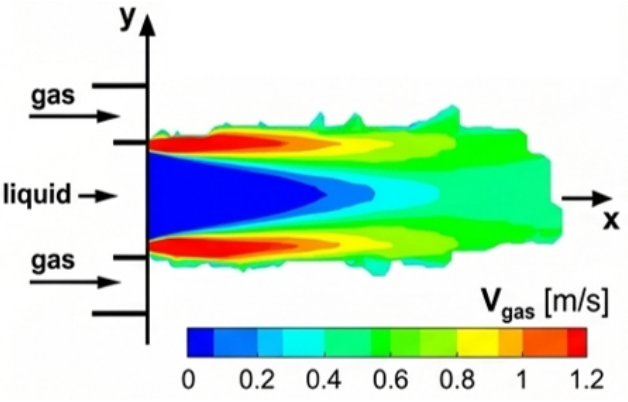


Figure 9 - Spatial distribution of the velocity magnitude of the carrier gas flow (v_{gas}) within the computational domain

Fig. 10 shows the spatial distribution of the relative velocity modulus between the gas and liquid phases in a two-dimensional axisymmetric computational domain. This parameter characterizes phase-slip intensity and drives interphase interactions.

The maximum values of relative velocity, reaching 0.5-0.6 m/s (red and orange zones), are localized in a narrow shear layer at the contact boundary of the high-speed gas flow and the biodiesel jet directly behind the nozzle exit. In this region, extreme velocity gradients develop, triggering surface hydrodynamic instabilities (such as Kelvin-Helmholtz instabilities) that govern droplet fragmentation and secondary breakup efficiency.

As the flow moves along the x-axis, the kinetic phase mismatch decreases, reflected in a monotonic drop in the relative velocity modulus (transitioning to green and blue regions with minimum values of 0-0.1 m/s) due to velocity-profile equalization and turbulent dissipation.

Fig. 11 shows the spatial distribution of turbulent kinetic energy (TKE) in a two-dimensional axisymmetric computational domain. This parameter characterizes the intensity of fluctuating motions and the level of local hydrodynamic fluctuations within the flow.

The maximum TKE values, ranging from 0.08 to 0.1 J/kg (indicated by red and orange zones), are clearly localized within narrow regions of intense shear at the interfaces between the high-velocity gas jets and the central liquid flow, immediately downstream of the nozzle exit. Extreme velocity gradients drive high turbulence generation in this region.

As the flow moves along the x-axis, turbulent pulsation intensity decreases to intermediate values of 0.04-0.06 J/kg (green-yellow range) due to energy dissipation. In the inner region of the solid fuel core and in the far spray trail, TKE values are minimal, at 0-0.02 J/kg (blue zone). Developed turbulence in shear layers is a key factor that intensifies primary and secondary droplet breakup and facilitates high-quality interphase mixing of fuel and gas.

A comparative analysis with modern studies of spray hydrodynamics shows that the spatial attenuation of TKE matches patterns reported in [25], which show that increased liquid-phase viscos-

ity and density reduce the intensity of hydrodynamic pulsations in the nozzle shear layer. In pure RMEB100 biodiesel, the increased dynamic viscosity damps small turbulent eddies, narrowing the peak TKE zone compared with less viscous conventional diesel fuel. As noted in [26], which uses the segmental Eulerian-Lagrangian approach, accurately accounting for pulsation damping at the phase boundary is crucial for adequately predicting the spatial boundary of primary breakdown and the final dispersed composition of the droplets.

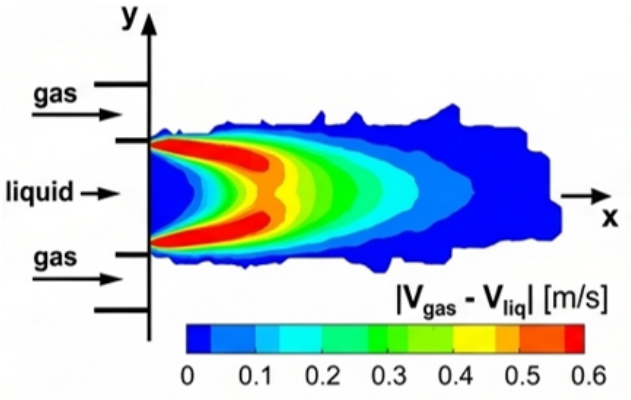


Figure 10 - Field of relative phase velocity gradients in zones where shear stresses develop

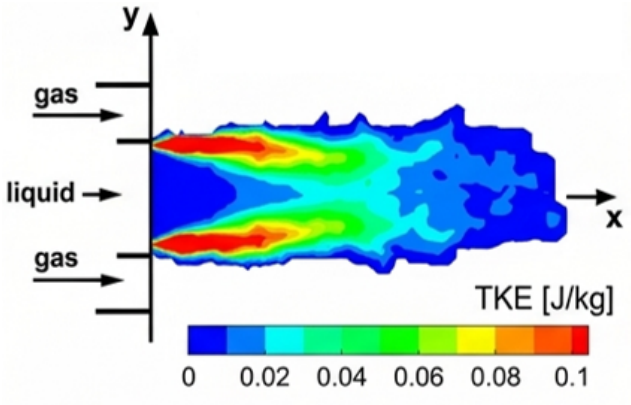


Figure 11 - Spatial distribution of turbulent kinetic energy (TKE) in the computational domain of a two-phase flow

Fig. 12 presents numerical modeling results of dispersed-phase dynamics within an Eulerian-Lagrangian framework, illustrating the kinematic and spatial-structural characteristics of the droplet flow.

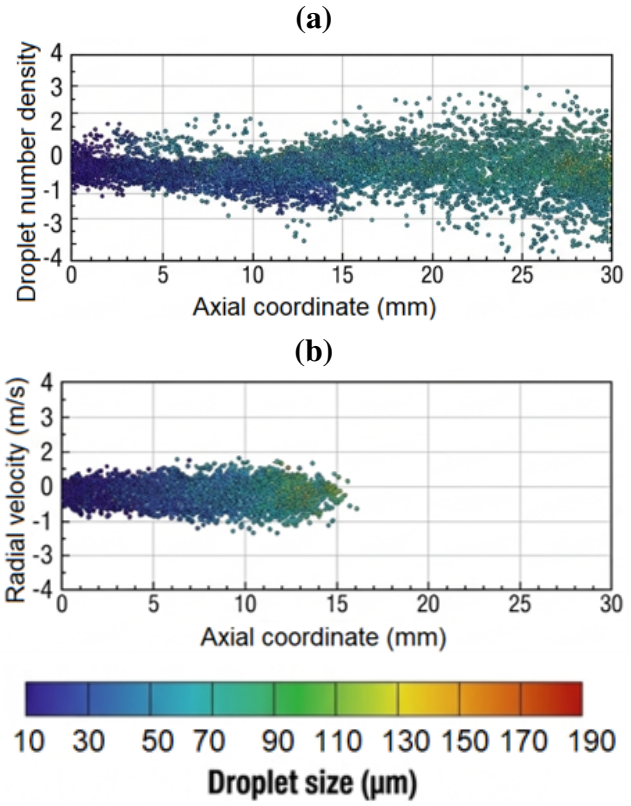


Figure 12 - Spatial distributions of droplet parameters: (a) droplet number density, (b) radial velocity magnitude, with the corresponding droplet size scale

Fig.12 a shows the distribution of the radial component of the droplet velocity as a function of axial coordinate (0-30 mm). The radial velocity values are mainly localized around 2 m/s, indicating moderate transverse divergence of the jet. The color indicates droplet size and reflects the evolution of the polydisperse composition: large droplets (130-170 μm, orange-red range) concentrate in the initial section of intense jet disintegration (x=10-15 mm), where secondary fragmentation has not yet completed. The finely dispersed fraction (10-15 μm, violet-blue tones) has higher kinetic mobility and is uniformly distributed throughout the torch volume.

Fig.12 b shows the spatial coverage and local density of the droplet ensemble along the flow direction. As the distance from the nozzle exit increases (x>15 mm), the droplet scattering region expands significantly due to intense turbulent transfer and aerodynamic entrainment

by carrier gas. The increase in the number of detected discrete elements in these downstream regions quantitatively confirms the cascade-like process in which large-scale liquid fragments undergo secondary breakup into smaller droplets.

CONCLUSIONS

Based on two-dimensional axisymmetric Eulerian-Lagrangian modeling of the coaxial air-blast atomization of biodiesel (RMEB100), the key hydrodynamic and structural-kinematic patterns governing the formation of the two-phase spray plume have been established:

1. Hydrodynamics and interphase interaction: High-velocity airflow (1.0–1.2 m/s) in the peripheral channels creates extreme velocity gradients and interphase slip (0.5–0.6 m/s) at the nozzle exit (x=0). This leads to the localized generation of high turbulent kinetic energy (TKE up to 0.1 J/kg) and triggers Kelvin-Helmholtz surface instabilities, which initiate the jet breakup mechanism;

2. Evolution of the continuous phase: In the near-nozzle zone, an extended, quasi-monolithic liquid fuel core (liquid volume fraction, L.V.F. $\approx$ 1) persists. Under the influence of aerodynamic shear stresses and turbulent mixing, this core undergoes wave formation and subsequent disintegration into dispersed elements;

3. Dispersed composition and SMD: Large droplets and liquid fragments (500–1000 μm) are localized within the peripheral high-shear zones in the initial region (x=10–15 mm). As a result of secondary fragmentation along the flow axis, a finely dispersed fraction (SMD=0-100 μm) is formed at the spray front and outer boundaries of the torch, which provides optimal conditions for interphase mass transfer and completeness of subsequent combustion;

4. Dispersed phase kinematics: Lagrangian tracking of the droplet flow demonstrates moderate transverse divergence of the jet (radial velocities within 2 m/s) with a significant expansion of the scattering zone at distant sites (x>15 mm) due to turbulent transport and aerodynamic entrainment by the carrier gas medium.

Detailed data on the spatial distribution of the Sauter mean diameter (SMD) of droplets, turbulent kinetic energy, and velocity fields enable engineers to address the following practical challenges:

- Based on identified zones of intense shear and regions where instabilities develop, the dimensions and configuration of coaxial air and fuel supply channels can be precisely adjusted. This helps minimize the energy required for pressurization while maintaining a high degree of atomization;

- Accurate knowledge of the localization of fine-droplet fractions and zones of active interphase mass transfer makes it possible to predict and reduce areas of incomplete fuel combustion, thereby lowering emissions of products of incomplete combustion and toxic compounds.

- Understanding the mechanisms of radial spray divergence and the entrainment of droplets into the carrier gas flow helps in designing the geometry of flame tubes in a way that prevents large droplets from reaching the combustion chamber walls, thereby avoiding burn-through;

- The developed and verified numerical model can serve as a "digital twin" of the atomizer, enabling the rapid testing of various operating parameters (pressure, temperature, air velocity) without the need for costly and time-consuming physical experiments.

The practical significance of the obtained results lies in their application in the design and optimization of front-end devices and combustion chamber structures of gas turbine engines (including aircraft gas turbine engines and stationary power plants) operating on biodiesel (RME B100). The obtained data enables precise calculation of the geometry of coaxial pneumatic nozzles, which helps minimize hydraulic losses, reduce energy costs for spraying, align combustion zones to reduce toxic emissions, and optimize flame spreading. This prevents large droplets from striking the walls of the combustion liners, which in turn avoids thermal burnout and extends the service life of the engine.

Despite the high accuracy and physical adequacy of the implemented approach, its limita-

tions are associated with the adopted thermodynamic assumptions in the Lagrangian description of the dispersed phase. In particular, multicomponent biodiesel (RME B100) is represented by an equivalent single-component surrogate with averaged characteristics, and the interphase heat and mass transfer is modeled in the approximation of uniform droplet temperature without taking into account fractional evaporation. Nevertheless, these modeling assumptions do not compromise the validity of the identified hydrodynamic principles governing the atomization process.

Promising areas for further research include expanding the modeling to include multicomponent surrogate biodiesel blends, investigating the effects of various fuel additives on atomization and evaporation processes, and integrating detailed kinetic mechanisms for the formation of harmful emissions, including soot, carbon and nitrogen oxides.

Author Contributions: Sh.O.: Conceptualization, Formal analysis, Writing–original draft, Supervision; G.K.: Methodology, Software; G.P: Data Curation; G.Sh.: Writing – review & editing, Visualization; A.A.: Resources, Investigation; K.R.: Investigation, Validation. All authors have read and agreed to the published version of the manuscript.

References

[1] Energy Institute, "Statistical review of world energy." London, 2024. https://www.energyinst.org/statistical-review

[2] International Energy Agency (IEA), "Global energy review: CO_2 emissions in 2023–2025." International Energy Agency, Paris, Tech. Rep., 2025. https://www.iea.org/reports/global-energy-review

[3] Argonne National Laboratory (ANL, USA), "The greenhouse gases, regulated emissions, and energy use in technologies (GREET) model." 2024. https://greet.es.anl.gov/

[4] International Energy Agency, "Transport sector fuel shares and energy outlook." International Energy Agency, Paris, Tech. Rep., 2024. https://www.iea.org/topics/transport

[5] International Energy Agency (IEA), "Renewables 2024–2025: Analysis and forecast to 2030." International Energy Agency, Paris, Tech. Rep., 2024. https://www.iea.org/reports/renewables

[6] Askarova, A., S. Bolegenova, S. Ospanova, K. Bolegenova, and A. Nurmukhanova. "Energetic efficiency of turbulent biofuel combustion for advanced bioenergy technologies." *International Journal of Mathematics and Physics* 16, no. 1 (2025): 20–28. https://doi.org/10.26577/ijmph.20251612

[7] Aminjan, K. K., M. Ghodrat, M. Heidari, A. Arjmandfard, P. Rahmanivahid, R. D. C. Pecho, Y. Yasin, and S. S. Abdullaev. "Study on duplex air-blast atomizers spray in the engine real operation conditions." *Physics of Fluids* 35, no. 7 (2023): 073326. https://doi.org/10.1063/5.0153468

[8] Kardos, R. A., E. Rácz, M. Malý, J. Jedelský, and V. Józsa. "Detailed spray analysis of airblast atomization of various fuels in a reacting environment." *International Journal of Heat and Mass Transfer* 227 (2024): 125548. https://doi.org/10.1016/j.ijheatmasstransfer.2024.125548

[9] Lamoot, L., B. Manescau, K. Chetehouna, and N. Gascoin. "Review on the effect of the phenomenon of cavitation in combustion efficiency and the role of biofuels as a solution against cavitation." *Energies* 14, no. 21 (2021): 7265. https://doi.org/10.3390/en14217265

[10] Ospanova, S., A. Askarova, S. Bolegenova, K. Bolegenova, and A. Nurmukhanova. "Simulation of the effective distribution of biofuel droplets in a reacting flow." *Journal of Machine Engineering* 25, no. 2 (2025): 123–137. https://doi.org/10.36897/jme/204226

[11] Lasheras, J. C. and E. J. Hopfinger. "Liquid jet instability and atomization in a coaxial gas stream." *Annual Review of Fluid Mechanics* 32, no. 1 (2000): 275–308. https://doi.org/10.1146/annurev.fluid.32.1.275

[12] Koshanova, A., G. Partizan, B. Mansurov, B. Medyanova, M. Mansurova, B. Aliev, and X. Jiang. "Synthesis of carbon nanostructures on iron nanopowders." *Journal of Physics: Conference Series* 741, no. 1 (2016): 012017. https://doi.org/10.1088/1742-6596/741/1/012017

[13] Nakysbekov, Z., B. Zhumadilov, B. Medyanova, G. Partizan, G. Suyundykova, and B. Aliev. "Synthesis of two-dimensional nanostructures at low temperatures." *International Journal of Mathematics and Physics* 16, no. 1 (2025): 41–46. https://doi.org/10.26577/ijmph.20251614

[14] Oruganti, S. K. and M. A. Gorokhovski. "Stochastic models in the under-resolved simulations of spray

formation during high-speed liquid injection." *Physics of Fluids* 36, no. 5 (2024): 052105. https://doi.org/10.1063/5.0206826

[15] Cleary, M. J., B. Wang, Z. Chi, and P. Li. "Modelling and simulation approaches for turbulent spray atomisation and combustion." *Applications in Energy and Combustion Science* 24 (2025): 100364. https://doi.org/10.1016/j.jaecs.2025.100364

[16] Zhong, W., Z. Xin, L. Wang, and H. Liu. "Investigations on high-speed flash boiling atomization of fuel based on numerical simulations." *Computer Modeling in Engineering & Sciences* 139 (2024): 1427–1453. https://doi.org/10.32604/cmes.2023.031271

[17] Jabbarzadeh Ghandilou, A. and H. Taghavifar. "New insight into air/spray boundary interaction for diesel and biodiesel fuels under different fuel temperatures." *Biofuels* 13, no. 9 (2022): 1087–1101. https://doi.org/10.1080/17597269.2022.2105867

[18] Li, H., M. Jia, R. Ding, X. Li, Z. Zhang, and Y. Zhang. "An improved kelvin-helmholtz rayleigh-taylor (kh-rt) breakup model with wide fuel applicability based on data-driven techniques." *Energy* 334 (2025): 137661. https://doi.org/10.1016/j.energy.2025.137661

[19] Bolegenova, S., A. Askarova, N. Slavinskaya, S. Ospanova, A. Maxutkhanova, A. Aldiyarova, and D. Yerbosynov. "Statistical modeling of spray formation, combustion, and evaporation of liquid fuel droplets." *Physical Sciences and Technology* 9, no. 3–4 (2022): 69–82, https://doi.org/10.26577/phst.2022.v9.i2.09.

[20] Liu, M., C. Jiang, B. C. Khoo, H. Zhu, and G. Gao. "A cell-based smoothed finite element model for the analysis of turbulent flow using realizable k-ε model and mixed meshes." *Journal of Computational Physics* 501 (2024): 112783. https://doi.org/10.1016/j.jcp.2024.112783

[21] Gorokhovski, M. and M. Herrmann. "Modeling primary atomization in sprays." *Annual Review of Fluid Mechanics* 40 (2008): 343–366. https://doi.org/10.1146/annurev.fluid.40.111406.102200

[22] Qi, X., Z. Jia, F. Zhang, G. Cao, Y. Ban, Y. Pei, L. Li, and P. Wang. "Study on the atomization mechanism and characteristics of liquid-liquid coaxial swirling injector with secondary injection." *Acta Astronautica* 249, no. Part A (2026): 1–15. https://doi.org/10.1016/j.actaastro.2026.07.007

[23] El Marnissi, Y. and J. Hwang. "Microscopic imaging on diesel spray and atomization process." *Processes* 12, no. 2 (2024): 359. https://doi.org/10.3390/pr12020359

[24] Aydogdu, M. "Analysis of the effect of rigid vegetation patches on the hydraulics of an open channel flow with realizable k-ε and reynolds stress turbulence models." *Flow Measurement and Instrumentation* 94 (2023): 102477. https://doi.org/10.1016/j.flowmeasinst.2023.102477

[25] Wang, X., H. Li, G. Li, J. Fan, H. Bai, Y. Gao, and H. Huo. "Effect of injection pressure on low-temperature fuel atomization characteristics of diesel engines under cold start conditions." *International Journal of Multiphase Flow* 169 (2023): 104612. https://doi.org/10.1016/j.ijmultiphaseflow.2023.104612

[26] Liu, Y. and D. L. Hung. "Segment-based eulerian–lagrangian transition method for primary and secondary atomization of viscous liquid jets." *International Journal of Multiphase Flow* 172 (2024): 104712. https://doi.org/10.1016/j.ijmultiphaseflow.2023.104712

Information about authors

Shynar Ospanova *– PhD, Acting Assoc.Prof., Almaty Technological University, Almaty, Kazakhstan, e-mail: s.osspanova@gmail.com*

Gulnaz Karybayeva *– Cand.Phys.-Math.Sci., Acting Assoc.Prof., Almaty Technological University, Almaty, Kazakhstan, e-mail: g.karybaeva@atu.edu.kz*

Gulmaira Partizan *– PhD, Deputy Chairman of the Management Board, Joint-Stock Company "National Center of Space Research and Technology", Almaty, Kazakhstan, e-mail: g.partizan@spaceres.kz*

Gulnur Shinikulova *– M.Sc., Senior Lecturer, Almaty Technological University, Almaty, Kazakhstan, e-mail: gulnur.shynykulova@gmail.com*

Aitkul Aldibekova *– M.Tech., Senior Lecturer, Almaty Technological University, Almaty, Kazakhstan, e-mail: aldibekova.a.n.@gmail.com*

Karashash Rustemova *– Cand.Phys.-Math.Sci., Assistant professor, Almaty Technological University, Almaty, Kazakhstan, e-mail: krustemova@list.ru*